

Secular and orbital variability of Cir X-1 observed in optical spectra

Helen M. Johnston,^{1*}, Kinwah Wu^{1,2}, Rob Fender³ and Jason G. Cullen¹

¹*Research Centre for Theoretical Astrophysics, School of Physics, University of Sydney, NSW 2006, Australia;*

²*Mullard Space Science Laboratory, University College London, Holmbury St Mary, Dorking, Surrey RH5 6NT;*

³*Astronomical Institute ‘Anton Pannekoek’, University of Amsterdam, Kruislaan 403, 1098 SJ Amsterdam, The Netherlands*

Received:

ABSTRACT

We have observed variations in the optical emission lines from the X-ray binary Circinus X-1. These variations may be attributed both to orbital variations and to long term secular changes in line strength. We have detected double-peaked H α emission lines on two occasions, providing the first direct evidence for an accretion disk in the system. The separation of the peaks was different on the two occasions, suggesting that the disk might have a different size. The equivalent width of the emission lines dropped by more than a factor of three between 1999 and 2000; this continues the trend seen in earlier data, so that the H α equivalent width has now declined by a factor of twenty since 1976. The emission lines do not appear to show signature of orbital motion, except for the data taken near phase 0, which show a significant velocity shift.

We have observed an absorption component to the He I lines on one occasion. We suggest that, unlike the P Cygni profiles seen in X-ray spectra, this absorption does not arise in the accelerating zone of a radiatively driven wind. Instead, the absorption arises in material previously ejected from the system. It was only seen on this one occasion because the strength of the emission line had dropped dramatically.

Key words: binaries: spectroscopic – stars: individual: Cir X-1 – stars: X-rays

1 INTRODUCTION

Cir X-1 is a highly unusual X-ray binary, whose nature has been a puzzle for many years. Since the early 1970s, Cir X-1 has shown erratic X-ray properties: its light curve differed dramatically each time it was observed. Nevertheless, there is a periodic modulation of 16.6 d (Kaluzienski et al. 1976), which is believed to be the orbital period of the binary. The compact star in Cir X-1 is a neutron star, inferred from the Type I X-ray bursts observed in a brief episode (Tennant, Fabian & Shafer 1986). Further support is provided by the Z-source behaviour seen recently in X-ray timing data from the *Rossi XTE* satellite (Shirey, Bradt & Levine 1999).

The radio counterpart of Cir X-1 is located 25' from the centre of the supernova remnant G321.9–0.3, and is apparently connected to the remnant by a radio nebula (Haynes et al. 1986). It shows flares at the same period as the X-ray modulation (Haynes et al. 1978). Cir X-1 has two arcminute-scale radio jets (Stewart et al. 1993), and an arcsecond-scale asymmetric jet suggests the presence of relativistic outflow from the source (Fender et al. 1998). The close association

of Cir X-1 with the supernova remnant suggests that the system may be a young ($< 10^5$ y old) runaway system from a supernova explosion (Stewart et al. 1993).

The optical counterpart to Cir X-1 was identified as a highly-reddened star with strong H α emission (Whelan et al. 1977). This object was later shown to consist of three stars within a radius of 1'.5, the southernmost of which is the true counterpart (Moneti 1992; Duncan et al. 1993). In 1997, we obtained spectra of Cir X-1 near apastron[†], using the Anglo-Australian Telescope (Johnston, Fender & Wu 1999, hereafter Paper I). We detected an asymmetric H α line which can be decomposed into two components, a narrow one and a broad component which is blue-shifted with respect to the narrow component. Comparison with archival spectra from the AAT and from HST showed that an asymmetric emission line has been present for the past twenty years. No previous observations have seen any evidence of an accretion disk.

In this paper, we report on new optical spectroscopic observations of Cir X-1 obtained during 1999 and 2000.

* E-mail: H.Johnston@physics.usyd.edu.au; kw@mssl.ucl.ac.uk; rpf@astro.uva.nl; J.Cullen@physics.usyd.edu.au

[†] Here and throughout, we use the words “periastron” and “apastron” to refer to phase 0 and phase 0.5 respectively, as calculated from the timing of the radio flares (Stewart et al. 1991).

Table 1. Journal of observations of Cir X-1. The columns show the UT date of observation, the Julian date of the midpoint of the observation, the telescope and instrument used, the mean phase of the observation, the total exposure time, and the wavelength range and resolution of the spectra, as measured from the arc lines. The phase was calculated according to the ephemeris of Stewart et al. (1991).

UT Date	JD	Instrument	Phase	t_{exp} (s)	Wavelength range (Å)	Resolution (Å)
1999 Jul 11	2451371.045	2.3m + DBS	0.880	18900	5600–7500	2.7
1999 Aug 20	2451410.910	2.3m + DBS	0.292	5400	5400–7330	2.1
1999 Aug 21	2451411.870	2.3m + DBS	0.350	1800	5400–7330	2.1
1999 Aug 22	2451412.901	2.3m + DBS	0.411	7200	5400–7330	2.1
2000 May 16	2451681.045	AAT + RGO	0.622	28800	5660–7000	1.3
2000 May 22	2451687.063	2.3m + DBS	0.985	28800	5570–7000	2.4
2000 Jul 12	2451738.096	2.3m + DBS	0.073	12600	5580–7510	4.8
2000 Jul 13	2451739.013	2.3m + DBS	0.129	19800	5508–7510	4.5

2 OBSERVATIONS AND DATA REDUCTION

Cir X-1 was observed on multiple occasions during 1999 and 2000, using the Double Beam Spectrograph (DBS) on the ANU 2.3-m telescope, and the RGO Spectrograph on the 3.9-m AAT. A complete log of observations is given in Table 1.

The 2000 May 16 observations were carried out with the RGO spectrograph in combination with the MITLL3 chip and a grating with 1200 grooves mm^{-1} , resulting in a dispersion of 1.3 Å pixel^{-1} . All other observations were carried out using the DBS with the standard SITe 1752×532 CCD with a 600 grooves mm^{-1} grating. The very red colour of the source means that no significant signal was detected in the blue arm of the DBS. Series of 1800 s object exposures were interspersed with CuAr arc-lamp exposures. A slit width of 1.5 or 2 arcsec was used, and the slit was always oriented north-south so that both Cir X-1 and star 2 of Moneti (1992) were in the slit. The spatial scale on the detector was $0''.91$ for the DBS and $0''.48$ for the RGO, which means the spectrum of Cir X-1 was confused with that of star 2; keeping the same slit orientation means that at least this contribution was constant. Because our previous work (Paper I) had shown no significant features associated with star 2, we have not attempted to remove its contribution from the spectrum.

The phases of the observations are shown in Table 1, as calculated from the ephemeris of Stewart et al. (1991), based on the timing of the radio flares. It can be seen that, while there is moderately good coverage of a range of orbital phases, there is a year separating the earliest spectra from the last spectra, so there are potential secular variations which may confuse any features arising from the orbital variation.

The IRAF software suite was used to remove the bias and pixel-to-pixel gain variations from each frame. As we had multiple consecutive observations of the same object, cosmic ray events were removed using the technique described by Croke (1995), as implemented in FIGARO. The wavelength calibration was performed in IRAF by fitting a low-order polynomial to the arc line wavelengths as a function of pixel number; the rms scatter of the fits was typically better than 0.1 pixel.

3 RESULTS

The spectra all show a strong $\text{H}\alpha$ emission line; the shape however changed significantly between the various observations. We can see both long-term secular variation, in the equivalent widths of the lines, and variations which seem to be correlated with the orbital phase of the observations, in the line-profile morphology. Unfortunately, with sparse orbital coverage, it is difficult to disentangle the latter from the former. Only with observations within a single orbit, and repeated observations at the various orbital phases, will we be able to be certain about some of the phenomena we describe here. However, with that caveat in mind, we will describe the data at hand.

3.1 $\text{H}\alpha$ line shape

As was seen in previous observations (Paper I), the $\text{H}\alpha$ line shows multiple components. In particular, the spectrum taken on 1999 July 11 shows a clear double-peaked profile. Such profiles are well known in the optical spectra of soft X-ray transients and cataclysmic variables, where they are usually taken to indicate the presence of an accretion disk (Smak 1981). A natural interpretation for the double-peaked lines in our spectra would therefore be that there is an accretion disk present, although other possible interpretations are discussed below (§ 4.3). This is the first time evidence of the accretion disk has been seen in the optical spectra of Cir X-1.

We fit Gaussian profiles to the $\text{H}\alpha$ line, using the `specfit` package in IRAF (Kriss 1994). After normalising each spectrum by a low-order polynomial fit to the continuum, we fit either two or three gaussians to the $\text{H}\alpha$ line. The spectrum taken on 1999 July 11 clearly showed a double-peaked profile, in addition to the broad blue-shifted component, so we fit three gaussians to this spectrum. The reduced χ^2_ν for $\nu = 85$ degrees of freedom changes from $\chi^2_\nu = 4.9$ for a two-gaussian fit to $\chi^2_\nu = 1.1$ for three gaussians. The spectrum from 2000 May 16 also required an extra narrow component to achieve a good fit ($\chi^2_\nu = 1.52$ for a two-gaussian fit, $\chi^2_\nu = 1.23$ for three gaussians). The other spectra were fit with two gaussians. The details of the fits are listed in Table 2.

The data and the fits are shown in Figure 1, with the spectra arranged in order of phase. Despite the spectra having been taken over a span of more than a year, there appears

Table 2. Fits to the emission line profiles. Column 2 shows the mean phase of the observation, column 3 shows the total equivalent width of the H α line $W_{\lambda,t}$, measured by direct summation of pixels in the emission line, and columns 4 and 5 show the equivalent width of the He I $\lambda 6678$ and $\lambda 7065$ lines, measured from Gaussian fits to the line profiles (see Sect. 3.3). The He I lines in the 2000 May 16 spectra show P Cygni profiles; the equivalent widths listed are those of the emission component. Columns 6–11 show the results of Gaussian fits to the H α line. The spectra for 1999 July 11 and 2000 May 16 were fit with three components, the other spectra with two. The fits are shown in Figure 1.

UT Date	Phase	$W_{\lambda,t}$	W_{λ}	W_{λ}	H α narrow component(s)			H α broad component		
		H α (\AA)	$\lambda 6678$ (\AA)	$\lambda 7065$ (\AA)	velocity (km s^{-1})	FWHM (km s^{-1})	W_{λ} (\AA)	velocity (km s^{-1})	FWHM (km s^{-1})	W_{λ} (\AA)
1999 Jul 11	0.880	81	3.5 ± 0.4	4.7 ± 0.3	-104 ± 10	270 ± 16	21 ± 2	-600 ± 40	550 ± 70	9.1 ± 1.1
1999 Aug 20	0.292	80	4.6 ± 0.9	6.7 ± 1.0	270 ± 10	400 ± 15	40 ± 1.5			
1999 Aug 21	0.350	79	1.7 ± 1.0	4.4 ± 0.8	261 ± 8	490 ± 20	47 ± 4	-90 ± 60	1010 ± 60	27 ± 4
1999 Aug 22	0.411	83	3.2 ± 0.8	3.9 ± 0.6	350 ± 16	290 ± 40	24 ± 6	180 ± 30	675 ± 50	51 ± 6
					330 ± 10	320 ± 24	30 ± 5	1040 ± 30	690 ± 30	49 ± 5
2000 May 16	0.622	12.2	0.28 ± 0.08	0.66 ± 0.09	-30 ± 5	210 ± 40	2.7 ± 0.7	-420 ± 30	630 ± 45	6.6 ± 0.9
					200 ± 5	170 ± 30	3.1 ± 0.7			
2000 May 22	0.985	10.1	1.4 ± 0.2	0.3 ± 0.1	87 ± 15	270 ± 60	1.5 ± 0.5	44 ± 18	1000 ± 50	9.5 ± 0.5
2000 Jul 12	0.073	25.0	2.0 ± 0.5	1.9 ± 0.3	307 ± 80	580 ± 60	11 ± 15	-20 ± 400	740 ± 230	10 ± 15
2000 Jul 13	0.129	26.3	2.6 ± 0.5	2.3 ± 0.4	290 ± 40	440 ± 40	13.8 ± 3	-115 ± 70	460 ± 80	8.0 ± 3

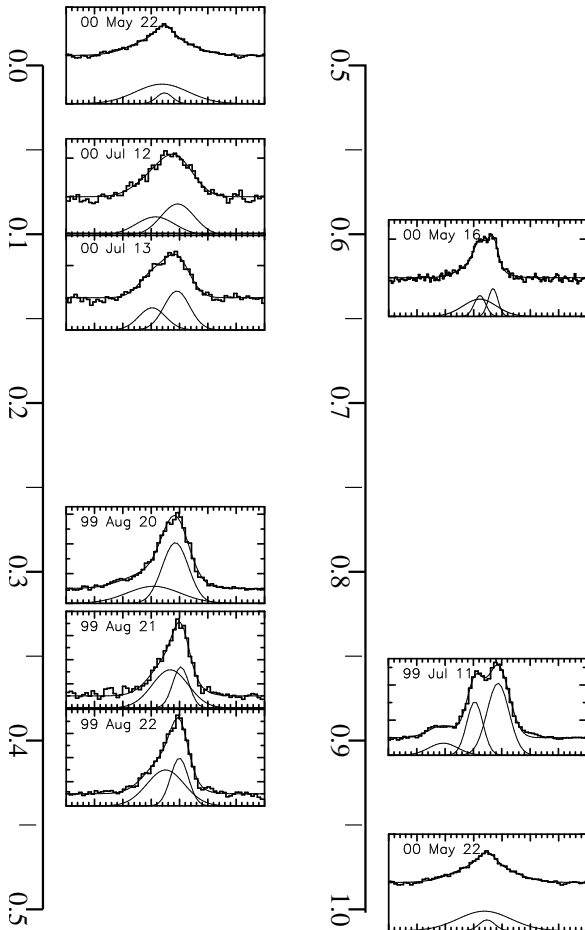


Figure 1. Line profiles of H α , showing the Gaussian fits to the lines and their sum. The spectra have been normalised by a polynomial fit to the continuum. The spectra are shown in order of phase, with the spectrum taken at phase 0 (1999 May 22) repeated at phase 1 for clarity. The spectrum at phase 0 is symmetric, with a broad component on the blue wing appearing at phases 0.1–0.5. At phase 0.6 the line appears to be double-peaked (or flat-topped?), while clear double peaks are seen at phase 0.9.

to be a clear trend of line shape with orbital phase. The spectrum taken at phase 0 (2000 May 22) is the only completely symmetric profile. At small phases, the line profile begins to show asymmetry in the line. Sometime after phase 0.4, the line shows a second peak in addition to the broad component (2000 May 16), which persists for the second half of the orbit (1999 July 11). We have fit two narrow components to the line at phase 0, although it is possible that the profile is flat-topped instead of intrinsically double-peaked. We will discuss the implications of this in Section 4.3.

In Paper I we presented five archival spectra from the AAT and one from HST; we can re-examine these spectra for evidence of the same pattern in the line profiles. Three spectra (1976 May, 1978 August and 1997 June) were taken near apastron, at phases 0.54, 0.52 and 0.51; none of them shows a double-peaked profile. The spectra taken in the first half of the orbit all show an asymmetry on the blue wing; no spectra were taken during the second half of the orbit (phases 0.6–0.9), so we do not know whether the double-peaked line has been consistently present. The spectrum taken near periastron (1977 September, phase 0.95) does not show a symmetric profile; the line is still asymmetric on the blue wing. Thus we can say very little about the persistence of the pattern we find in our spectra from 1999–2000.

3.2 Secular variation in H α equivalent width

The equivalent width W_{λ} of the H α line is shown in Table 2 and its evolution is plotted in Figure 2. The equivalent width dropped dramatically between 1999 (MJD 51370–51412) and 2000 (MJD 51680–51738), from 80 \AA to 25 \AA , and the drop is independent of the phase of the observations. This drop coincides with a drop in the X-ray flux observed by *RXTE*, where the baseline flux between flares ($\sim 100 \text{ ct s}^{-1}$ for the All-Sky Monitor (ASM) on *RXTE*) began a slow decline around 2000 March (MJD 51600). This downward trend of the H α equivalent width is consistent with the trend seen over the last 25 years (Paper I, Table 2), where the observations in 1976 May found $W_{\lambda} = 580 \text{\AA}$, declining to 120 \AA in 1997. Rough flux-calibration of this data

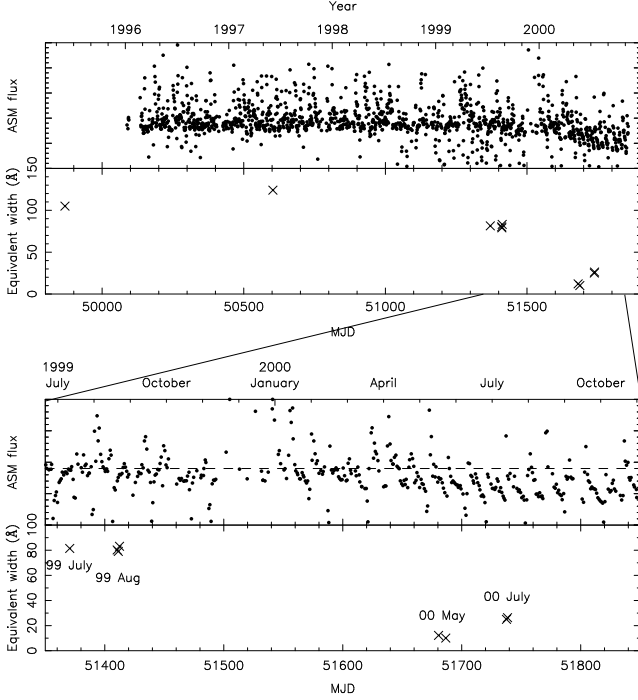


Figure 2. Variation of the X-ray flux and equivalent width of the $H\alpha$ line with time. The top section of each panel shows the 1-day average ASM flux measured by XTE, the lower section shows the equivalent width of the $H\alpha$ line. The entire RXTE/ASM light curve for Cir X-1 is shown in the top panel, while an expanded version of the light curve since 1999 is shown in the bottom panel. The “baseline” X-ray flux, between flares and dips, began to decline from a value of about 1.2 Crab (shown by the dashed line) to 0.7 Crab by 2000 July (MJD 51740). The $H\alpha$ equivalent widths for 1995 (phase 0.18) and 1997 (phase 0.51) are from Paper I. The drop is independent of phase.

and the archival data shows that this change in the equivalent width is not due to an increase in the brightness of the continuum, and therefore must reflect a real and dramatic decrease in the brightness of the emission line.

3.3 He I lines

The spectra all show emission lines of He I $\lambda 6678$ and $\lambda 7065$. In most cases, these lines are quite faint; the equivalent width of the He I lines also dropped dramatically between 1999 and 2000. We measured the equivalent width of the lines by fitting Gaussians in the same manner as for the $H\alpha$ lines. For most of the spectra, a single gaussian for each line was sufficient. For the 1999 July 11 lines, the He I lines were double peaked just like the $H\alpha$ line. The 1999 August 20 line required two components for a satisfactory fit.

The spectrum from 2000 May 16 clearly showed P Cygni profiles in both the He I lines (Figure 3). P Cygni profiles were recently discovered in X-ray spectra of Cir X-1 taken by *Chandra* (Brandt & Schulz 2000). The peak-to-valley distance of the profile in the optical spectra is 7.62 \AA , or 340 km s^{-1} . This is a much smaller velocity than that seen in the X-ray spectra ($2000\text{--}3000 \text{ km s}^{-1}$).

Figure 4 shows the equivalent width of the He I lines as a function of phase. In order to remove the dramatic

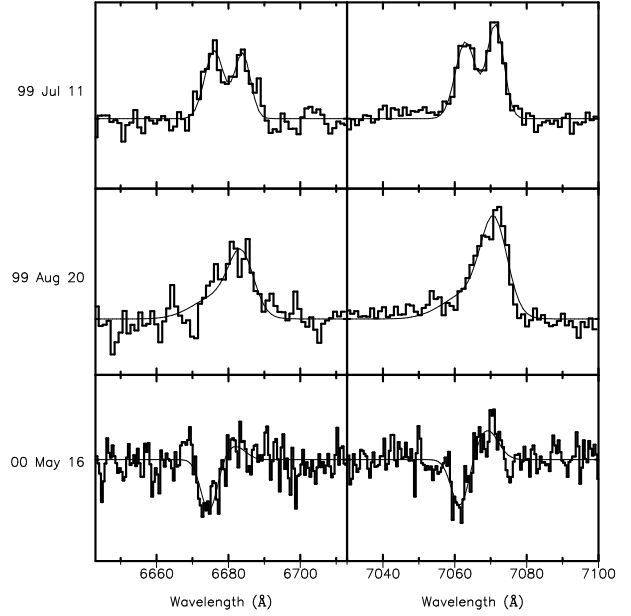


Figure 3. Selected line profiles of He I, showing the fits to the lines. The spectra have been normalised by a polynomial fit to the continuum; the wavelengths of the fits were constrained to have the same velocity and width. The left side of the figure shows the $\lambda 6678$ line, the right side the $\lambda 7065$ line. The 1999 July 11 spectrum shows a double-peaked profile, the 1999 August 20 spectrum shows an asymmetric line, and the 2000 May 16 spectrum shows a P Cygni profile.

secular variation which occurred between 1999 and 2000, we normalised the He I equivalent widths by the equivalent width of the $H\alpha$ line (Table 2, column 3). The results show a smooth variation with phase; both transitions are of similar strength, except for the abrupt reversal in the phase 0 spectrum, when the $\lambda 7065$ line becomes significantly weaker than the $\lambda 6678$ line.

3.4 Velocities of the emission lines

The measured velocities of the emission line do not seem to conform to any sensible pattern. In particular, there is no discernible signature of orbital motion over most of the orbit. This implies that the site of the emission is changing throughout the orbit, and possibly over the one year spanning our observations – see Section 4 for a discussion of the implications for a model for the system.

However, we do see significant orbital motion in the data taken near periastron. We divided the data taken on 2000 May 22 into four equal segments of 7200 s duration and performed the same analysis on each segment. The results are shown in Fig. 5. Both components of the $H\alpha$ line, as well as the He I $\lambda 6678$ line (not plotted), show an increase in velocity of 120 km s^{-1} over six hours. This certainly implies that at this point in the orbit the emission line is tracking the orbital motion; in a highly elliptical orbit, nearly all the velocity swing happens right near periastron (Tauris et al. 1999).

With only four velocity points, we cannot place any interesting constraints on the orbital parameters. Two representative curves are plotted with the observed points; it

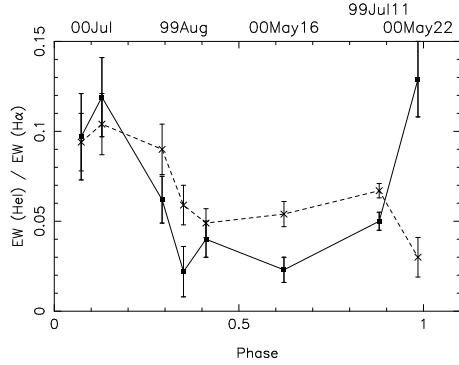


Figure 4. Equivalent width of the He I lines, normalised by the H α equivalent width, as a function of phase. The filled squares show He I λ 6678, the crosses He I λ 7065. The dates of the observations are indicated above the plot. The spectrum at phase 0.62 (2000 May 16) showed P Cygni profiles in the He I lines: only the equivalent width of the emission component has been plotted here, thus underestimating the intrinsic line strength.

can be seen that there is essentially no constraint on the orbital inclination, though the eccentricity must be high to produce the observed sharp swing in velocity.

3.5 Timing of periastron

It is important to note that the phases have been calculated using the ephemeris of Stewart et al. (1991). Phase 0 refers to the onset of radio flares, and how this relates to the X-ray dips observed by *RXTE* is not clear. We have examined the quick-look results provided by the *RXTE*/ASM team to see if we can compare the observed times of the X-ray dips with the predicted times from the Stewart et al. ephemeris. The periastron passage on 2000 May 22 did not have good ASM coverage; both the preceding and the following X-ray dips appear to have occurred 0.4–0.5 d later than the phase 0 predicted by the Stewart et al. ephemeris, corresponding to a shift of 0.024–0.03 in phase. Given that the ephemeris was based on radio flares, and that the X-ray light curve changes so dramatically, this agreement is reasonably good. In future work we hope to further investigate the exact relationship between the X-ray, radio and optical behaviour.

4 DISCUSSION

4.1 A model for the system

In Paper I, we proposed a theoretical model for Cir X-1. The binary is a low-mass neutron-star binary with an ultra-eccentric binary orbit ($e \gtrsim 0.7$, possibly as high as 0.9; Tauris et al. 1999). During periastron passage, the companion star (which is a subgiant of about 3–5 M_{\odot}) overfills its Roche-lobe, causing a transfer of mass at a super-Eddington rate, which in turn drives a strong matter outflow. After periastron, mass transfer from the companion ceases, but accretion continues at a near-Eddington rate as the neutron star captures the residual matter in its Roche-lobe. An accretion disk gradually forms, which is initially non-Keplerian and geometrically thick. This change between quasi-spherical and disk accretion causes the change between

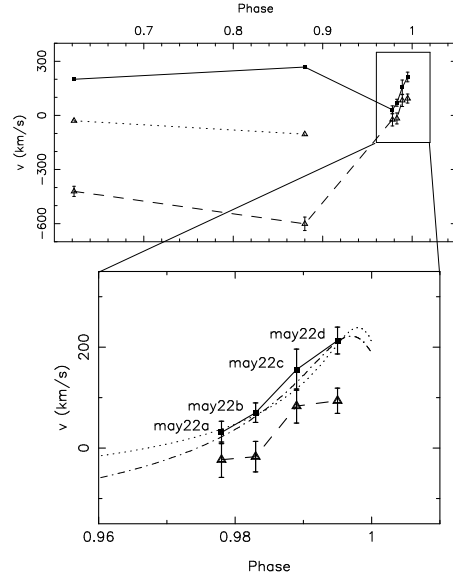


Figure 5. Velocities of the fitted components near phase 0. The data from 2000 May 22 has been divided into four spectra of duration 7200 s; the rapid swing of velocity in both the narrow (solid line) and broad (dashed line) components is evident in the expanded section to the lower right. The dotted line shows the second narrow (blueward) peak in the double-peaked spectra on 99 July 11 and 2000 May 16. The dotted and dot-dashed lines show two representative orbital curves, assuming $M_1 = 1.5 M_{\odot}$, $M_2 = 3.0 M_{\odot}$; the dotted line has $i = 45^\circ$, $e = 0.9$, while the dot-dashed line has $i = 85^\circ$, $e = 0.87$; both curves have the longitude of periastron set to 210° and a systemic velocity of -120 km s^{-1} and -220 km s^{-1} respectively.

strong X-ray variability after phase 0. Between phases 0.5–0.9, the accretion disk becomes Keplerian and there is steady accretion. The disk is then disrupted by tidal forces during the following periastron passage.

Based on the consistently high velocities seen in all the data up to that time, we suggested in Paper I that Cir X-1 might have a very high radial velocity. Our new spectroscopic data do not show evidence of high line-of-sight velocities, though the argument about the velocity from the association with G321.9–0.3 is still valid.

4.2 Sites of emission

Our data and the archival data show a persistent broad component in the H α line, indicating the presence of a high-velocity flow. One possibility for the line-formation region is the accretion flow close to the neutron star. The X-ray luminosity of Cir X-1 reaches the Eddington limit at the phases shortly after periastron. This implies a mass accretion rate $\dot{M} \gtrsim 2 \times 10^{18} \text{ g s}^{-1}$. The quantity $n_e R^2$ is given by

$$n_e R^2 \approx 1.0 \times 10^{33} \left(\frac{\dot{M}}{2 \times 10^{18} \text{ g s}^{-1}} \right) \times \left(\frac{1000 \text{ km s}^{-1}}{v} \right) \chi^{-1} \text{ cm}^{-1}, \quad (1)$$

where n_e is the electron number density. χ parametrises the degree of spherical accretion, and its value is unity for spherical accretion. Hence the ionisation parameter

$$\xi \equiv \frac{L_x}{n_e R^2} \sim 10^5 \chi^{-1} \quad (\text{in cgs units}), \quad (2)$$

implying a temperature $T \sim 10^7$ K for the accreting matter (see Hatchett et al. 1976). The strong X-ray emission from the source would therefore completely ionise the accretion gas with inflowing velocity with $v \sim 1000 \text{ km s}^{-1}$, making it unlikely to emit H Balmer lines.

Alternatively, the broad component of the $\text{H}\alpha$ line could be emitted from the outflow matter. A characteristic of a radiatively driven outflow is that the outflowing matter is accelerated from a slow initial velocity and eventually reaches a terminal velocity. As there is a negative gradient from the observer to the outflow matter, the blue wing of the line suffers very strong self-absorption. The line would therefore show a P Cygni profile. Since our optical data do not show the P Cygni profile typical of such a radiatively driven outflow (with the exception of one set of spectra: see below), the gradient of the line-of-sight velocity in the line formation region must be positive, i.e. the outflow is decelerating. If the broad component originates from a high-velocity outflow, the line formation region is in the decelerating zone, and the accelerating zone is behind the photosphere. Such outflow might be caused by an ejection of high-velocity material during the violent mass transfer epoch at the periastron.

On one occasion, we do see an absorption component in the blue wing of the He I lines, though not in the $\text{H}\alpha$ line. We suggest that, instead of arising in a radiatively driven outflow, we are seeing absorption from the outflowing material far from the system, superimposed on emission lines from the accretion disk. The absorbing matter consists of material ejected from the system in previous episodes of violent mass transfer, and the absorption is occurring at some distance from the system, where the outflow has decelerated significantly from the $2000\text{--}3000 \text{ km s}^{-1}$ seen in the X-ray spectra.

The absorption is seen only in spectra from 2000 May 16, which is when the He I emission from the disk was weakest (Table 2). We suggest that the absorption in the outflow is masked in the other spectra by the strength of the emission line, which is also why we do not see similar absorption in the $\text{H}\alpha$ line.

4.3 First detection of an accretion disk?

Our detection of the double-peaked lines formed in an accretion disk is strong evidence for the eccentric binary model for Cir X-1. The double-peaked lines were seen twice, in spectra taken almost a year apart, at phases 0.88 and 0.62. Spectra taken in the first half of the orbit all show an asymmetric $\text{H}\alpha$ emission line, while the spectrum taken at periastron (phase 0.98) shows a completely symmetric line.

Double-peaked lines are often found in cataclysmic variables (e.g. IP Peg, see Marsh 1988), which are binaries with a white dwarf accreting material from a low-mass companion star, and in black-hole binaries during the high-soft state (e.g. GX339-4, see Soria, Wu & Johnston 1999) or quiescence (e.g. A0620-00, Johnston, Kulkarni & Oke 1989). They are also found in the accretion-disk corona sources (e.g. 2A 1822-371, Mason et al. 1982). They are, however,

rare amongst other X-ray binaries, and X-ray pulsars do not typically show double-peaked optical lines[‡].

It was shown (Wu et al. 2001) that double-peaked lines can be formed in a temperature-inversion layer on an opaque accretion disk when the disk is irradiated by soft X-rays. The X-ray spectrum of Cir X-1 is soft, dominated by a black-body component with an effective temperature $T \sim 2 \text{ keV}$ (Shirey et al. 1999b). Thus the double-peaked lines observed in Cir X-1 probably indicate the presence of an accretion disk. Moreover, a significant part of the disk surface is not obscured from the central X-ray source so that the irradiatively induced temperature inversion can occur.

It is interesting to note that the 1999 July (Fig. 1, phase 0.88) observation, which was the first spectrum to show double-peaked lines, was taken in the cycle after an orbit during which Cir X-1 did not have a post-periastron X-ray flare; only a handful of orbits observed by XTE had not shown such a flare before then. It is possible that this has some bearing on the visibility of the optical lines from the accretion disk, for instance if the absence of an X-ray outburst means that matter which usually obscures the disk was more transparent than usual. Alternatively, the accretion rates during this observational epoch were low enough to allow a mature Keplerian disk to develop within an orbital cycle.

The double-peaked lines seen in 2000 May (Fig. 1, phase 0.62) did not occur after such an anomalous orbit. However, by that stage the X-ray flux observed by *RXTE* had begun to drop (see Sec 3.2, Fig. 2), which might also imply that veiling material was thinner.

It is possible that, instead of being an intrinsically double-peaked line, the profile observed on 2000 May 16 is actually flat-topped. Such lines have been seen in several black hole candidates, such as GX 339-4 (Smith et al. 1999; Soria et al. 1999) and GRO J1655-40 (Soria et al. 2000), where they are interpreted as arising in a horizontal wind launched from a disk (Murray & Chiang 1997). Possibly the line in Cir X-1 arises in a similar fashion; however, this requires the emission site to change from a spherical outflow (phases < 0.5 ; Fig. 1) to a horizontal wind (phase 0.6) to a disk (phase 0.88). The interpretation of the line as a barely-resolved double peak has at least the virtue of being a simpler explanation.

Assuming the double-peaked lines arise in an accretion disk, then the separation reflects the velocity at the outer edge of the emission region of the accretion disk (Smak 1981). The separation of the peaks was very different on the two occasions the double-peaked profile was observed (370 km s^{-1} in 1999 July, 230 km s^{-1} in 2000 May), which suggests that the accretion disk had a very different size. This could be due to the different phase of the observation, implying the disk is shrinking as periastron approaches. Figure 6 shows a comparison between the observed peak separations and a model where the size of the disk is truncated by the size of the Roche lobe in an eccentric orbit. This represents the largest possible size for the accretion disk, and hence a *lower* limit to the separation of the two peaks. The fact that the observed velocities are above this limit implies

[‡] Though note that 2A 1822-371 was recently shown (Jonker & van der Klis 2001) to be an X-ray pulsar!

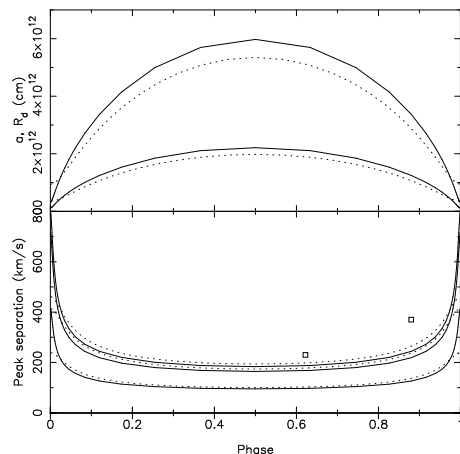


Figure 6. Sketch of the separation of the double-peaks as a function of orbital phase, for some representative orbital parameters, compared with our observed values. The top panel shows the separation between the two stars (top line) and the outer radius of the disk, where we assume the disk is limited by the size of the Roche lobe of the compact star and its outer radius is truncated at $0.7 R_L$. The masses of the two stars are $M_1 = 1.5 M_\odot$, $M_2 = 3.0 M_\odot$, and the orbital eccentricity and inclination are $e = 0.9$ (solid lines) and $e = 0.7$ (dotted lines). The bottom panel shows the predicted peak separation for such a disk, for a range of orbital inclinations: (from the bottom) $i = 30$ deg, 45 deg and 75 deg. The open squares show the measured peak separation for the two dates on which they were observed.

that either the disk has not reached the truncation radius, or that the emission region for $H\alpha$ is not at the outer edge of the disk. The former would imply that, after the disk is disrupted at periastron, it has not had time to grow to the truncation radius before the Roche lobe begins to contract again (Fig. 6), which would imply that the viscous timescale for the growth of the disk is longer than the dynamical timescale, which is 8 d for half an orbit.

Alternatively, the change in peak separation could be the result of a secular variation in the size of the emitting region; or the temperature of the disk could be varying, so that the location of the $H\alpha$ emission site is changing. In this case, the smaller peak separation implies a hotter disk, with the emission site having moved towards the outside of the disk.

Other explanations for the double-peaked profiles are possible which do not require the presence of an accretion disk. They could, for instance, arise in a bipolar jet, since a relativistic jet has been inferred from high-resolution radio maps of the source (Fender et al. 1998). However, in SS 433, which has a jet with velocity $\sim 0.3c$, the separation of the components is hundreds of angstroms (Margon 1984), compared to the $5\text{--}8 \text{ \AA}$ seen in our spectra. Such a small separation could only be produced by a relativistic jet if the jet was almost in the plane of the sky (in which case the transverse Doppler shift would cause both components to be redshifted). Thus any jet would need to be non-relativistic to produce the observed lines.

Variable double-peaked lines have also been seen in infrared spectra of Cyg X-3 (Fender et al. 1999), where they were interpreted as arising in a disk-like wind outside the binary orbit. Such a disk-wind requires a large angular mo-

mentum, which would be unlikely in a system like Cir X-1 with such a large orbital period. The double-peaks could arise from emission in different parts of the system; however, we note that the standard sites for such localised emission, such as the hot spot where the accretion stream impacts the disk, still require the presence of a disk in the system.

Finally, it is possible that the central dip in the double-peaked profile is formed by absorption in front between us and the emitter, especially given the fact that we see absorption in the He I lines on a different occasion (see § 3.3). Such lines are seen in symbiotic stars, such as CH Cygni, which shows two symmetric peaks separated by a deep central reversal (Anderson et al. 1980); in this object, the profile is assumed to arise in a self-absorbed wind. However, in the case of the profiles seen in Cir X-1, the conditions for such absorption would be hard to produce. Since the profile is symmetric, the absorbers would need to be at a very similar velocity to the emitters; and since the central dip is broad and does not reach the continuum, the absorbers would need a wide velocity dispersion and only a small optical depth. The most probable interpretation of the profile is that it arises from the Doppler motions in an accretion disk.

4.4 Long-term changes in the emission lines

The brightness of the emission lines has decreased dramatically over the past 25 years, from $W_\lambda = 580 \text{ \AA}$ in 1976 to 25 \AA in 2000. Our interpretation is that the contribution of different emission sites to the emission lines has been shifting over the years. The contribution from the accretion disk is likely to have been essentially constant, since the temperature of the disk is limited by the accretion rate (assumed to be at Eddington) and the size of the disk is limited by the size of the orbit. The contribution to the emission line from other regions – the outflow, the companion star – can change dramatically depending on the state of the system. It is possible that we have seen the disk for the first time precisely because the contributions from other sites in the orbit have lessened, so the $H\alpha$ line is now dominated by emission from the accretion disk.

ACKNOWLEDGMENTS

We thank the ANU RSAA Time Assignment Committee for their generous allocation of time to this project. We thank Roberto Soria for assistance with the observations. We also thank the referee for providing useful suggestions and clarifications, particularly for suggestions about the flat-topped profile. KW acknowledges the support from the ARC through an ARC Australian Research Fellowship. This work is partially supported by an ARC/USyd Sesqui R&D Grant.

REFERENCES

- Anderson, C. M., Oliverson, N. A., Nordsieck, K. H. 1980, *ApJ*, 242, 188
- Brandt, N., Schulz, N. S. 2000, *ApJ*, 544, L123
- Croke, B. F. W. 1995, *PASP*, 107, 1255
- Duncan, A. R., Stewart, R. T., Haynes, R. F. 1993, *MNRAS*, 265, 157

- Fender, R., Spencer, R., Tzioumis, T., Wu, K., van der Klis, M., van Paradijs, J., Johnston, H. 1998, *ApJ*, 506, L121
- Fender, R. P., Hanson, M. M., Pooley, G. G. 1999, *MNRAS*, 308, 473
- Hatchett, S., Buff, J., McCray, R. 1976, *ApJ*, 206, 847
- Haynes, R. F., Jauncey, D. L., Murdin, P. G. et al. 1978, *MNRAS*, 185, 661
- Haynes, R. F., Komesaroff, M. M., Little, A. G. et al. 1986, *Nat*, 324, 233
- Johnston, H. M., Fender, R. P., Wu, K. 1999, *MNRAS*, 308, 415 (Paper I)
- Johnston, H. M., Kulkarni, S. R., Oke, J. B. 1989, *ApJ*, 345, 492
- Jonker, P. G., van der Klis, M. 2001, *ApJ*, 553, L43
- Kaluzienski, L. J., Holt, S. S., Boldt, E. A., Serlemitsos, P. J. 1976, *ApJ*, 208, L71
- Kriss, G. A. 1994, in D. R. Crabtree, R. J. Hanisch, J. Barnes (eds.), *Astronomical Data Analysis Software and Systems III*, Vol. 61 of *ASP Conference Series*, ASP, San Francisco, p. 437
- Margon, B. 1984, *ARA&A*, 22, 507
- Marsh, T. R. 1988, *MNRAS*, 231, 1117
- Mason, K. O., Murdin, P. G., Tuohy, I. R., Seitzer, P., Branduardi-Raymont, G. 1982, *MNRAS*, 200, 793
- Moneti, A. 1992, *A&A*, 260, L7
- Murray, N., Chiang, J. 1997, *ApJ*, 474, 91
- Shirey, R. E., Bradt, H. V., Levine, A. M. 1999a, *ApJ*, 517, 472
- Shirey, R. E., Levine, A. M., Bradt, H. V. 1999b, *ApJ*, 524, 1048
- Smak, J. 1981, *Acta Astron.*, 31, 395
- Smith, I. A., Filippenko, A. V., Leonard, D. C. 1999, *ApJ*, 519, 779
- Soria, R., Wu, K., Hunstead, R. W. 2000, *ApJ*, 539, 445
- Soria, R., Wu, K., Johnston, H. M. 1999, *MNRAS*, 310, 71
- Stewart, R. T., Caswell, J. L., Haynes, R. F., Nelson, G. J. 1993, *MNRAS*, 261, 593
- Stewart, R. T., Nelson, G. J., Penninx, W., Kitamoto, S., Miyamoto, S., Nicolson, G. D. 1991, *MNRAS*, 253, 212
- Tauris, T. M., Fender, R. P., van den Heuvel, E. P. J., Johnston, H. M., Wu, K. 1999, *MNRAS*, 310, 1165
- Tennant, A. F., Fabian, A. C., Shafer, R. A. 1986, *MNRAS*, 221, 27p
- Whelan, J. A. J., Mayo, S. K., Wickramasinghe, D. T. et al. 1977, *MNRAS*, 181, 259
- Wu, K., Soria, R., Hunstead, R. W., Johnston, H. M. 2001, *MNRAS*, 320, 177